Chinese Chemical Letters 37 (2026) 112156

Contents lists available at ScienceDirect

Chinese Chemical Letters

journal homepage: www.elsevier.com/locate/cclet

Dual photocatalytic access to antiviral alkenyl phosphonates *via* radical 1,4-difunctionalization across ordinary alkenes and arylacetylenes

Ruihua Liu[a], Jiashu Chen[a], Nan Zhou[a], Cong Shi[a], Hongyun Qin[a], Wenlong Shan[a], Zemin Wang[a], Chenxia Gao[a], Chao Liu[a], Bokan Wang[c], Chao Xie[a], Xiangqian Li[a], Yuxi Lin[a], Jiqiang Zhu[a], Pan Xing[a], Dayong Shi[a,b,*]

[a] *State Key Laboratory of Microbial Technology, Shandong University, Qingdao 266237, China*
[b] *Shandong Lead High Biotechnology Co., Ltd., Ji'nan 250031, China*
[c] *Laboratory for Marine Drugs and Bioproducts, Qingdao Marine Science and Technology Center, Qingdao 266237, China*

ARTICLE INFO

Article history:
Received 8 July 2025
Revised 7 November 2025
Accepted 21 November 2025
Available online 22 November 2025

Keywords:
Radical 1,4-difunctionalization
Dual photocatalytic
Alkenyl phosphonates
Z/E selectivity
Alkenes
Arylacetylenes

ABSTRACT

The radical-mediated 1,2-difunctionalization of alkenes or alkynes has emerged as an efficient strategy for augmenting molecular diversity and complexity. Nevertheless, developing remote 1,4-difunctionalization reactions through radical cascade additions involving two intermolecular unsaturated bonds confronts complex chemo-, regio-, and stereoselectivity challenges. Here, we report a photocatalytic strategy that enables the first radical 1,4-difunctionalization across simple alkenes and arylacetylenes, leveraging the distinct reactivity between alkyl phosphites and different carbon radicals, by employing 1 mol% *fac*-$Ir(ppy)_3$ as the photocatalyst and quinuclidine as the base. Mechanistic studies reveal that the photoexcited $Ir(III)^*$ synergistically governs two processes: (1) Single-electron transfer (SET) activation of Rf-X to generate fluoroalkyl radicals, and (2) triplet energy transfer (TEnT)-mediated stereo-control of the constructed alkenyl phosphonates to achieve high *Z/E* selectivity. This method enables the efficient synthesis of various δ-fluoroalkyl-substituted alkenyl phosphonates with high *Z/E* selectivity under mild conditions. Furthermore, some products exhibit a synergistic inhibitory effect on porcine epidemic diarrhea virus (PEDV), effectively blocking viral adsorption and replication while preventing PEDV-induced cell apoptosis *in vitro*.

© 2026 Published by Elsevier B.V. on behalf of Chinese Chemical Society and Institute of Materia Medica, Chinese Academy of Medical Sciences.

Multicomponent reactions (MCRs), which combine three or more simple components into a complex molecule in one step, significantly enhance synthetic efficiency by reducing the number of steps and eliminating the need for intermediate isolation and purification [1–3]. This atom- and step-economical strategy holds great potential for advancing drug discovery by enabling the streamlined synthesis of structurally diverse compounds. However, the inherent complexity of MCRs introduces substantial challenges in achieving precise control over reaction selectivity [2,3]. The radical 1,2-difunctionalization of alkenes or alkynes is a well-established three-component reaction for creating molecules with neighboring functional groups [4–6]. However, harnessing radical stepwise addition to more than one unsaturated bond poses formidable challenges due to complex chemo-, regio-, and stereoselectivity issues [7,8]. To address these challenges, researchers have increasingly employed radical addition reactions involving carefully designed radical acceptors containing two or more unsaturated bonds [9,10]. This strategy has proven effective for synthesizing functionalized carbo- and heterocycles *via* radical intramolecular cyclization. Significant advances have recently been made in addition reactions mediated by radical polarity [11–16], which involve two intermolecular unsaturated bonds with pronounced electronic disparity (Fig. 1A) [17–25]. Notably, a series of radical 1,4-difunctionalization reactions, such as 1,4-oxyimination [17], carboimination [18,19], hydrooxygenation [20], hydroamination [21,22], dihydrogenation [23,24], and hydrotrifluoromethylation [25], have been developed *via* photocatalytic or transition-metal-catalyzed radical relay strategies. In these transformations, electrophilic radicals add preferentially to electron-rich alkenes, and the resultant nucleophilic alkyl radicals tend to react with other electron-deficient Michael-type alkenes or alkynes. Conversely, if the initiating radical is nucleophilic, the stepwise addition process proceeds in the reverse order [11–16]. Indeed, the radical 1,4-difunctionalization facilitated by radical polarity represents an efficient methodology for synthesizing highly functionalized

* Corresponding author.
E-mail address: shidayong@sdu.edu.cn (D. Shi).

https://doi.org/10.1016/j.cclet.2025.112156
1001-8417/© 2026 Published by Elsevier B.V. on behalf of Chinese Chemical Society and Institute of Materia Medica, Chinese Academy of Medical Sciences.

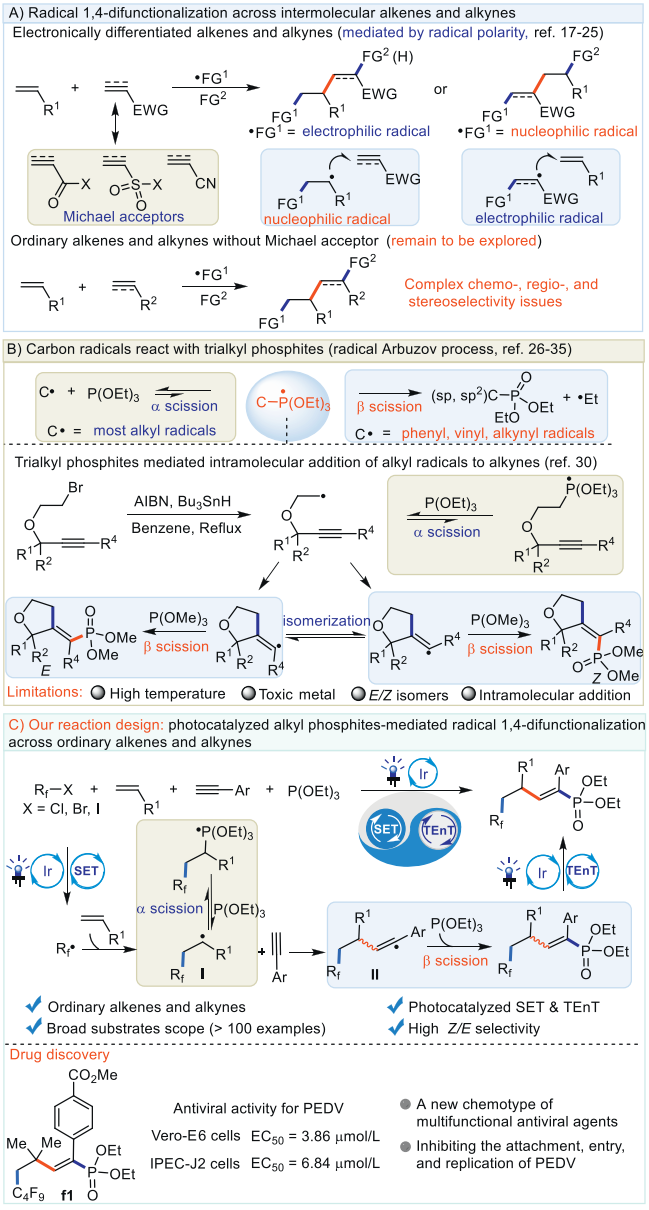


Fig. 1. Background and the present research.

molecules with high chemoselectivity. However, general strategies for achieving radical 1,4-difunctionalization across ordinary alkenes and alkynes lacking significant electronic disparity remain, to our knowledge, unreported.

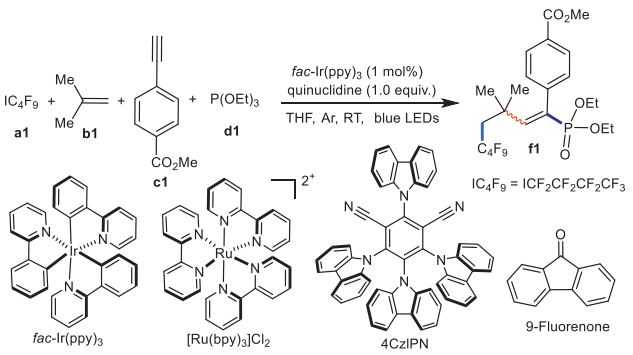
Phosphonates, as structural analogs of naturally occurring phosphates, exhibit diverse biological activities and have been widely utilized in developing antiviral, antimicrobial, and anti-inflammatory agents, among others [26,27]. The direct addition of carbon radicals to alkyl phosphites (radical Arbuzov process) presents a promising strategy for synthesizing functionalized phosphonates [28–35]. As depicted in Fig. 1B, different carbon radicals demonstrate distinct selectivity in the radical Arbuzov process [28–35]. Phenyl, vinyl, and alkynyl radicals selectively undergo β-scission of the resulting phosphoranyl radical upon reaction with $P(OEt)_3$, yielding delocalized phosphonates. In contrast, most alkyl radicals exhibit limited reactivity towards $P(OEt)_3$ due to the weaker C–P bond strength, leading to α-scission of the resulting phosphoranyl radical [28,29,35]. Exploiting this selectivity, the Bentrude group developed a pioneering work on the formation of cyclic vinylphosphonates through $P(OMe)_3$-mediated intramolecular addition of alkyl radicals to a carbon-carbon triple bond, followed by the trapping of more reactive vinyl radicals using $P(OMe)_3$ under thermal AIBN/Bu_3SnH conditions [30,31]. However, achieving control over the *Z/E* selectivity of this reaction poses challenges due to the steric hindrance of various substrates and the rapid isomerization of the resulting vinyl radicals [30,31,36–38]. Therefore, it is highly desirable to explore the alkyl phosphites-mediated intermolecular addition of alkyl radicals to alkynes, as well as the synthesis of functionalized vinylphosphonates with enhanced *Z/E* selectivity under mild reaction conditions.

Drawing inspiration from recent advancements in visible-light-photocatalyzed radical cascade reactions [39–48] and the radical Arbuzov process [28–35], we have developed the first photocatalytic alkyl phosphites-mediated radical 1,4-difunctionalization across ordinary alkenes and arylacetylenes (Fig. 1C). In this strategy, the photoexcited Ir(III)* facilitates the reduction of Rf-X, generating the fluoroalkyl radical Rf· *via* a SET process [47]. The resulting Rf·, a weak electrophilic radical, preferentially adds to alkenes rather than arylacetylenes, constructing a more stable nucleophilic alkyl radical **I** [11–16,49]. Although adding alkyl radical **I** to $P(OEt)_3$ is reversible due to the α-scission in the resulting phosphoranyl radicals, the situation changes when alkyl radical **I** adds to arylacetylenes. In this case, the resulting vinyl radical **II** is rapidly trapped by $P(OEt)_3$, forming the functionalized alkenyl phosphonates *via* the radical Arbuzov process [28–35]. The *Z/E* selectivity of the forming vinylphosphonates was further regulated by photoexcited Ir(III)* through the TEnT process [50–53]. A range of structurally diverse δ-fluoroalkyl-substituted alkenyl phosphonates with potential biological activities has been efficiently synthesized with exceptional *Z/E* selectivity by integrating photocatalyzed SET and TEnT processes. Furthermore, compared to ordinary phosphonates, fluoroalkyl-substituted phosphonates exhibit enhanced promise for pharmaceutical applications due to their improved efficiency, bioavailability, and metabolic stability [54].

The research on coronaviruses (CoVs) has garnered increasing attention in recent years, largely driven by the global impact of the coronavirus disease 2019 (COVID-19) pandemic. CoVs cause various diseases affecting animals' and humans' respiratory systems, gastrointestinal tract, liver function, and neurological health [55]. To accelerate antiviral drug discovery against rapidly mutating coronaviruses, chemists are developing novel synthetic strategies to generate structurally diverse molecules for drug screening. PEDV, a member of the α genus of the coronavirus family, infects pigs of all ages, leading to acute diarrhea, vomiting, dehydration, and a high fatality rate in piglets [56,57]. Porcine epidemic diarrhea (PED) has led to severe economic losses for the global pig industry due to its highly infectious nature and the absence of effective drugs and vaccines [58]. In the United States alone, over 7 million pigs were killed by PED between 2013 and 2014 [59]. Research also shows that PEDV can infect the cells of bats, monkeys, and even humans, indicating a potential threat to other species [60]. Current efforts in antiviral drug development focus on two primary strategies, inhibiting viral replication [61,62] and preventing viral entry into host cells [63,64]. While several small-molecule inhibitors specifically targeting viral replication [65,66] or entry [60,67,68] exhibit promising anti-PEDV activity, there remains a lack of efficient drugs available for clinical application. Given that viral entry and replication are critical steps in the transmission of the virus, developing novel multifunctional anti-PEDV agents capable of synergistically inhibiting these processes represents a promising direction for research

The four-component reaction was initiated by photoirradiating a mixture containing perfluorobutyl iodide **a1**, isobutylene **b1** at approximately 15 % concentration in THF, 4-ethynylbenzoicacidmethylester **c1**, triethyl phosphite **d1**, a photocatalyst,

Table 1
Optimization of reaction conditions.



Entry	Deviation from the standard conditions[a]	Yield (%)[b]	*E*/*Z*[c]
1	None	78	66:1
2	Et_3N instead of quinuclidine	59	45:1
3	DBU instead of quinuclidine	34	23:1
4	TMEDA instead of quinuclidine	58	60:1
5	DIPEA instead of quinuclidine	27	10:1
6	DEA instead of quinuclidine	46	12:1
7	CH_3CN and THF	23	39:1
8	DCE and THF	47	60:1
9	1,4-Dioxane and THF	43	55:1
10	$[Ru(bpy)_3]Cl_2$ instead of *fac*-Ir(ppy)$_3$	39	8:1
11	4CzIPN instead of *fac*-Ir(ppy)$_3$	57	18:1
12	9-Fluorenone instead of *fac*-Ir(ppy)$_3$	48	16:1
13	10 h	69	18:1
14	No light	0	-
15	No *fac*-Ir(ppy)$_3$	37	8:1
16	No quinuclidine	43	40:1

THF = tetrahydrofuran, DBU = 1,8-diazabicyclo[5.4.0]undec−7-ene, TMEDA = *N*,*N*,*N*′,*N*′-tetramethylethylenediamine, DIPEA = *N*,*N*-diisopropylethylamine, DEA = diethylamine, DCE = 1,2-dichloroethane.

[a] Conditions: **a1** (0.24 mmol), **b1** (0.5 mmol), **c1** (0.2 mmol), **d1** (0.6 mmol), quinuclidine (0.2 mmol), and *fac*-Ir(ppy)$_3$ was stirred in THF (0.21 mL) under Ar at room temperature for 48 h under the irradiation of blue LEDs.

[b] Isolated yields.

[c] The *E*/*Z* ratio of the products was determined by ^{1}H NMR spectroscopy.

and a base under Ar at room temperature. Pleasingly, the desired 1,4-difunctionalized product **f1** was isolated with a yield of 78 % and excellent *Z*/*E* selectivity using only 1 mol% of *fac*-Ir(ppy)$_3$ as the photocatalyst and quinuclidine under irradiation from blue LEDs (Table 1, entry 1). Screening various bases such as Et_3N, DBU, TMEDA, DIPEA, and DEA did not obtain better results in terms of either yield or stereoselectivity (Table 1, entries 2–6). Adding additional organic solvents like CH_3CN, DCE, and 1,4-dioxane decreased product yields (Table 1, entries 7–9). Other photocatalysts, including $[Ru(bpy)_3]Cl_2$, 4CzIPN, and 9-fluorenone, also catalyzed this multicomponent reaction; however, they yielded product **f1** with low *Z*/*E* selectivity (Table 1, entries 10–12). Shortening the reaction time compromised the *Z*/*E* selectivity of the product (Table 1, entry 13). The controlled experiments demonstrated that the reaction was light-dependent, with no product formation observed without light (Table 1, entry 14). Although the reaction proceeded in the absence of either a photocatalyst or a base, the yield of **f1** was dramatically reduced (Table 1, entries 15 and 16). Additionally, in the absence of a photocatalyst, the product exhibited poor *Z*/*E* selectivity (Table 1, entry 15), indicating the crucial role of the *fac*-Ir(ppy)$_3$ in regulating the configuration of the forming vinylphosphonates [50–53].

After determining the optimized reaction condition (Table 1, entry 1), we initially explored the substrate scope of arylacetylenes, as illustrated in Fig. 2. Simple phenylacetylenes bearing various valuable functional groups such as CO_2Me, COMe, CN, CF_3, F, Cl, Br, OCF_3, $CHMe_2$, and SO_2NH_2 with different substitution patterns (*para*-, *meta*-, and *ortho*-substitutions) readily underwent this multicomponent reaction to form the 1,4-difunctionalized products **f1**−**16** in moderate to good yields while exhibiting excellent *Z*/*E* selectivity. Notably, reactions involving electron-poor arylacetylenes yielded better yields than those with electron-rich counterparts. Interestingly, the *N*-ethylation product **f14** was formed using phenylacetylenes bearing $N(SO_2CF_3)_2$ group. The reaction also proceeded effectively with polysubstituted arylacetylenes, yielding desired products **f17** and **f18** in good yields with excellent *Z*/*E* selectivity. However, a moderate *Z*/*E* selectivity was observed when employing 1-ethynylnaphthalene (**f19**). Furthermore, this reaction occurred smoothly with a series of (hetero)arylacetylenes containing diverse heteroaryl moieties such as pyridine, pyrimidine, pyrazine, quinoline, thiophene, thiazole, and benzothiazole (**f20**–**41**). Consequently, this approach holds significant potential for discovering novel bioactive compounds characterized by distinctive structures due to the prevalent presence of such heterocyclic frameworks in drug entities. Specifically, 2-, 3-, and 4-ethynylpyridines adorned with various functional groups (F, Cl, Br, Me, OMe, and CO_2Me) at different positions were all well tolerated in the reaction, resulting in moderate to good yields of the desired products (**f20**–**32**). Most of these products synthesized from (hetero)arylacetylenes exhibited excellent *Z*/*E* selectivity; however, a mixture of *Z*/*E* isomers was observed only in three instances (**f20**, **f23**–**24**). In these three examples, the compromised *Z*/*E* selectivity likely arises from inadequate kinetic differentiation during the TEnT process, where energy is transferred from the photoexcited $[Ir(ppy)_3]^*$ to geometrically distinct *Z*/*E*-alkenyl phosphonates. Notably, when *fac*-Ir(diFppy)$_3$ was employed as the photocatalyst, products (**f20, f23–24**) were obtained with good *Z*/*E* selectivity. The synthetic potential of this strategy was further demonstrated through the successful application of a series of complex arylacetylenes that incorporate the frameworks of various biologically relevant natural products and pharmaceuticals. These include Estrone (**f42**), Thalidomide (**f43**–**44**), Vitamin E (**f45**), Dehydroabietylamine (**f46**), peptides (**f47**–**49**), Fructose (**f50**), Amoxapine (**f51**), and Fasudil (**f52**). Attempts using alkyl-substituted alkynes as substrates under identical conditions yielded no desired product (Fig. S2 in Supporting information). This diminished reactivity likely stems from inadequate stabilization of the vinyl radical intermediate, which lacks the crucial resonance stabilization provided by conjugated aromatic systems.

We subsequently investigated the general applicability of this protocol by examining a variety of unactivated alkenes, and the results were illustrated in Fig. 3. Simple terminal alkenes, whether linked to linear or cyclic alkyl frameworks, demonstrated good tolerance in this reaction, leading to the formation of the corresponding functionalized alkenyl phosphates with satisfactory yields and good *Z*/*E* selectivity (**f53**–**57**). The reaction was also effective with alkenes containing various functional groups, including ketone, ethers, esters, alcohols, and amides (**f58**–**67**). Interestingly, 4,4,5,5-tetramethyl-2-vinyl-1,3,2-dioxaborolane proved a suitable alternative to gaseous ethylene in this reaction pathway, forming deborylation products **f68**. In addition, the reaction proceeded smoothly when employing multi-substituted terminal or non-terminal alkenes as substrates (**f69**–**73**). This strategy was also applicable to the alkenes derived from various natural products and drugs such as (+)-Dihydrocarvone (**f74**), Valencene (**f75**), Nootkatone (**f76**), (-)-Menthol (**f77**), (1*R*)-(+)-Camphanic acid (**f78**), Isoborneol (**f79**), Indometacin (**f80**), Lbuprofen (**f81**), Adapalene (**f82**), Probenecid (**f83**), and Dihydrocholesterol (**f84**), which highlights the method's utility for late-stage modification of intricate natural products and drugs. Notably, when both terminal and non-terminal alkenes coexist within the same substrate, only the terminal alkenes demonstrate reactivity, while the internal alkenes remain unreactive (**f75**–**76**).

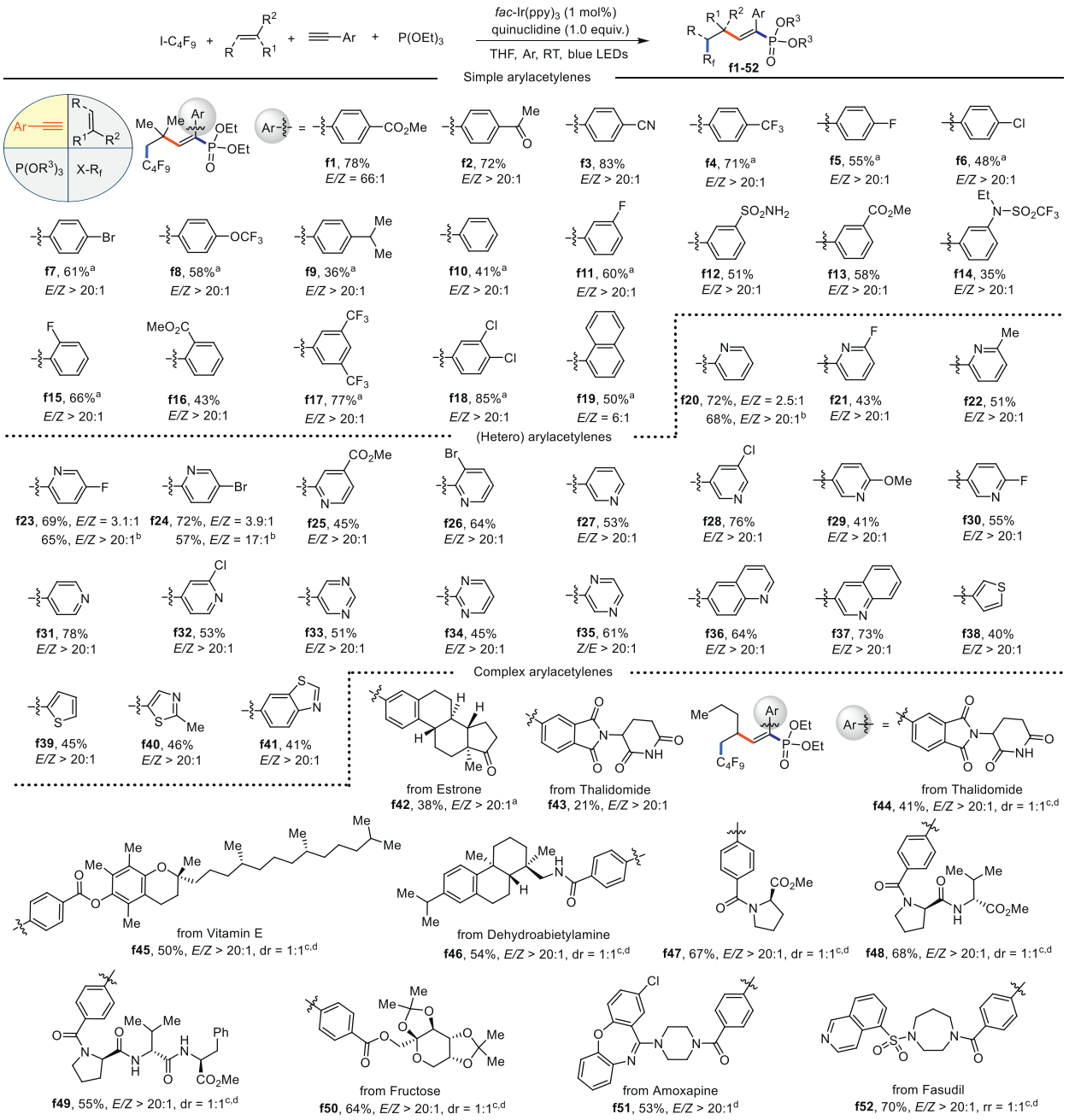


Fig. 2. Scope of arylacetylenes. Reaction conditions 1: perfluorobutyl iodide (0.24 mmol), alkenes (0.5 mmol), arylacetylenes (0.2 mmol), triethyl phosphite (0.6 mmol), *fac*-Ir(ppy)$_3$ (1 mol%), and quinuclidine (0.2 mmol) were stirred in THF and irradiated with blue LEDs under Ar at RT for 48 h. Isolated yields. The *Z*/*E* ratio was determined by ^{1}H NMR spectroscopy. [a] Triethyl phosphite (1.2 mmol) was used. [b] *fac*-Ir(diFppy)$_3$ was employed as the photocatalyst. [c] The diastereo ratio (dr) was determined by ^{31}P or ^{1}H NMR spectroscopy. [d] DCE (0.2 mL) was employed as the solvent, and the quantity of other reactants utilized was reduced by fifty percent.

We further examined the substrate compatibility of this radical multicomponent reaction by testing various alkyl phosphites and fluoroalkyl radical precursors. The reaction proceeded efficiently with alkyl phosphites attached to structurally diverse alkyl moieties, yielding 1,4-difunctionalized products with good yields and high *Z*/*E* selectivity (**f85**–**91**). In addition to trialkyl phosphites, monoaryl or diaryl substituted alkyl phosphites were also compatible with this methodology, enabling the synthesis of symmetric or asymmetric alkenyl phosphate esters in high yields (**f88**–**89**, **f91**). Beyond perfluorobutyl iodide, Togni's reagent II and other branched or linear perfluoroalkyl iodides with varying chain lengths reacted smoothly under this protocol, affording products **f92**–**95** in satisfactory yields and excellent *Z*/*E* selectivity. Furthermore, diverse difluorobromoacetic acid derivatives served as effective radical precursors for this reaction, synthesizing *δ*-difluoroalkyl-substituted alkenyl phosphates **f96**–**102**. This protocol also demonstrated versatility with other radical precursors, such as CF_3CH_2I and CCl_4, yielding 1,4-difunctionalized products **f103** and **f104**.

To elucidate the photoinitiation mechanism of this strategy, UV-vis absorption, Stern-Volmer experiments were carried out as shown in Fig. 4. It was observed that the reaction remained feasible in the absence of both a photocatalyst or quinuclidine, albeit with reduced efficiency (Table 1, entries 15 and 16). This finding suggests that the reaction may have followed two initiation pathways to generate fluoroalkyl radicals. One pathway involves the single-electron reduction of perfluorobutyl iodide by photoexcited

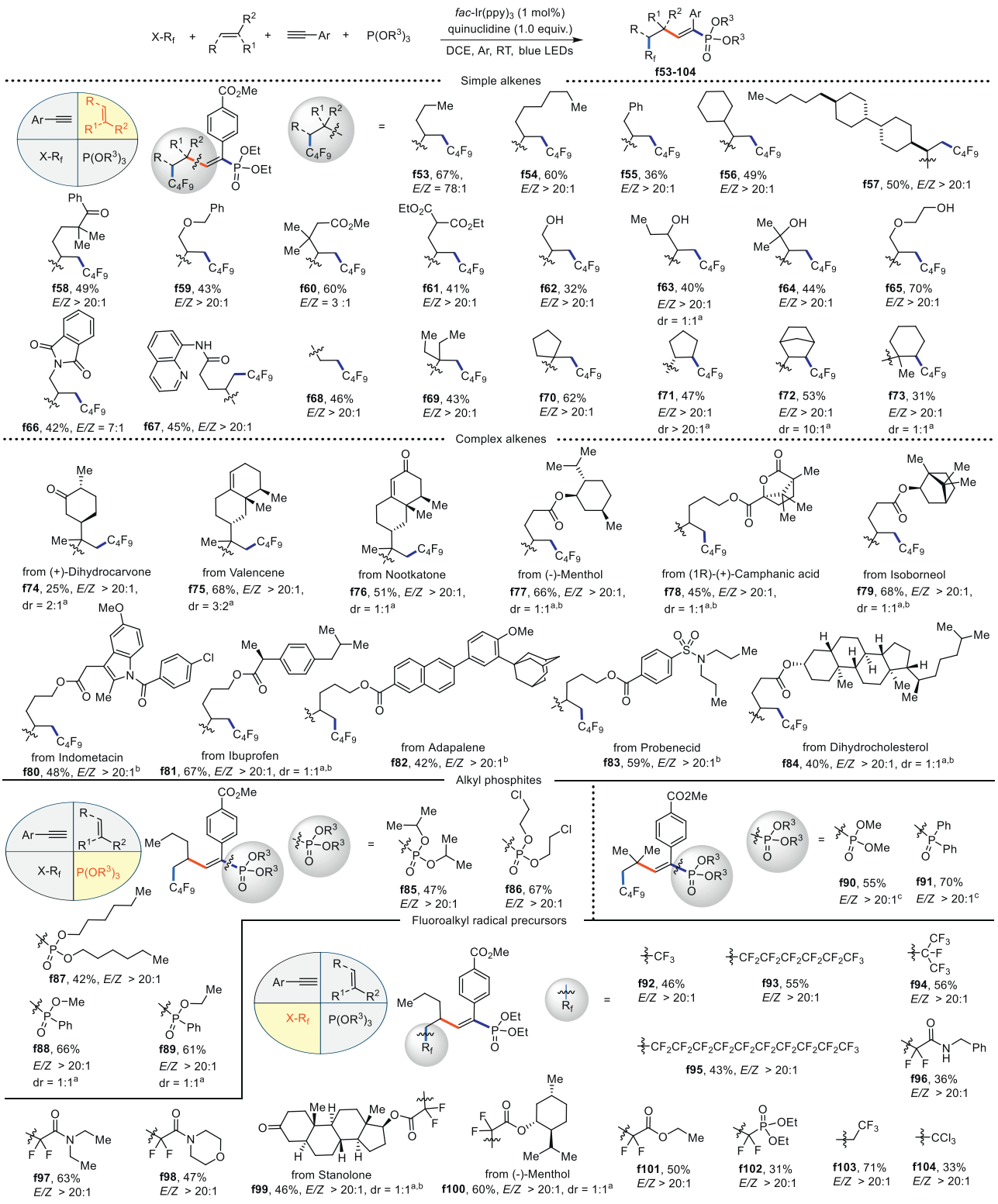


Fig. 3. Scope of alkenes, alkyl phosphites, and fluoroalkyl radical precursors. Reaction conditions 2: radical precursors (0.24 mmol), alkenes (0.5 mmol), arylacetylenes (0.2 mmol), triethyl phosphite (0.6 mmol), *fac*-Ir(ppy)$_3$ (1 mol%), and quinuclidine (0.2 mmol) were stirred in DCE (0.2 mL) and irradiated with blue LEDs under Ar at RT for 48 h. Isolated yields. The *Z*/*E* ratio was determined by isolated and ^{1}H NMR spectroscopy. [a] The *dr* was determined by ^{31}P or ^{1}H NMR spectroscopy. [b] DCE (0.2 mL) was employed as the solvent, and the quantity of other reactants was reduced by fifty percent. [c] The reaction condition was consistent with the standard reaction condition 1.

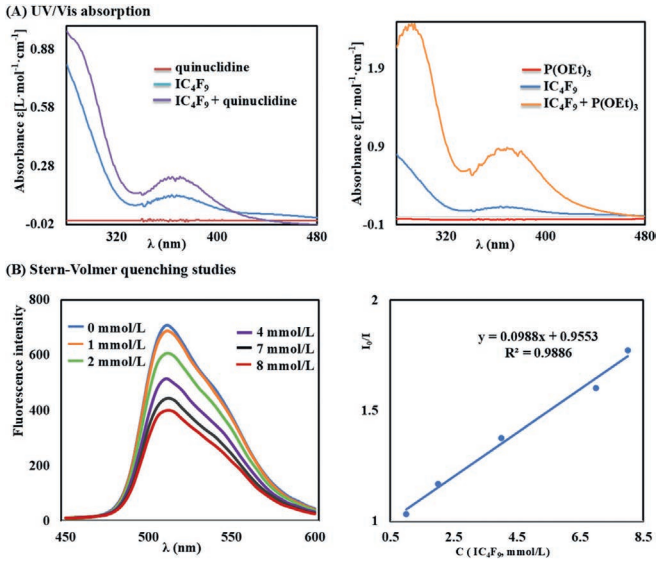


Fig. 4. Photoinitiation mechanism studies. (A) UV–vis absorption. (B) Stern-Volmer quenching studies.

Ir(III)* [47], while another pathway entails the photoinitiation of an EDA adduct formed from perfluorobutyl iodide and quinuclidine or $P(OEt)_3$ [69–71]. To confirm that the reaction proceeds *via* an EDA complex between fluoroalkyl iodides and quinuclidine or $P(OEt)_3$, UV–vis spectroscopy analysis was conducted (Fig. 4A). A red shift of IC_4F_9 were observed upon the addition of quinuclidine or $P(OEt)_3$. These results suggest that the EDA complexes are formed [69–71]. Moreover, fluorescence quenching experiments showed that the excited *fac*-Ir(III)* could be significantly quenched by fluoroalky iodides (Fig. 4B). Therefore, the radical initiation pathway also involves the single electron reduction between fluoroalkyl radical precursor and the photoexcited *fac*-Ir(III)* [47]. Furthermore, fluorescence quenching experiments, different quenching processes of alkyl radicals (Fig. S3 in Supporting information), and prior literature reports [47,72–73] collectively establish the involvement of a photoredox catalytic mechanism. Subsequent quantum yield determination revealed $\Phi = 2.2$, indicating the concurrent involvement of a radical chain process. Crucially, light/dark experiments (Fig. S4 in Supporting information) showed complete termination of 1,4-difunctionalized product formation upon irradiation cessation, demonstrating the transient nature of this radical chain.

To further elucidate the reaction mechanism of this strategy, control experiments, radical trapping experiment, and radical probe experiment were carried out as shown in Fig. 5. The sub-

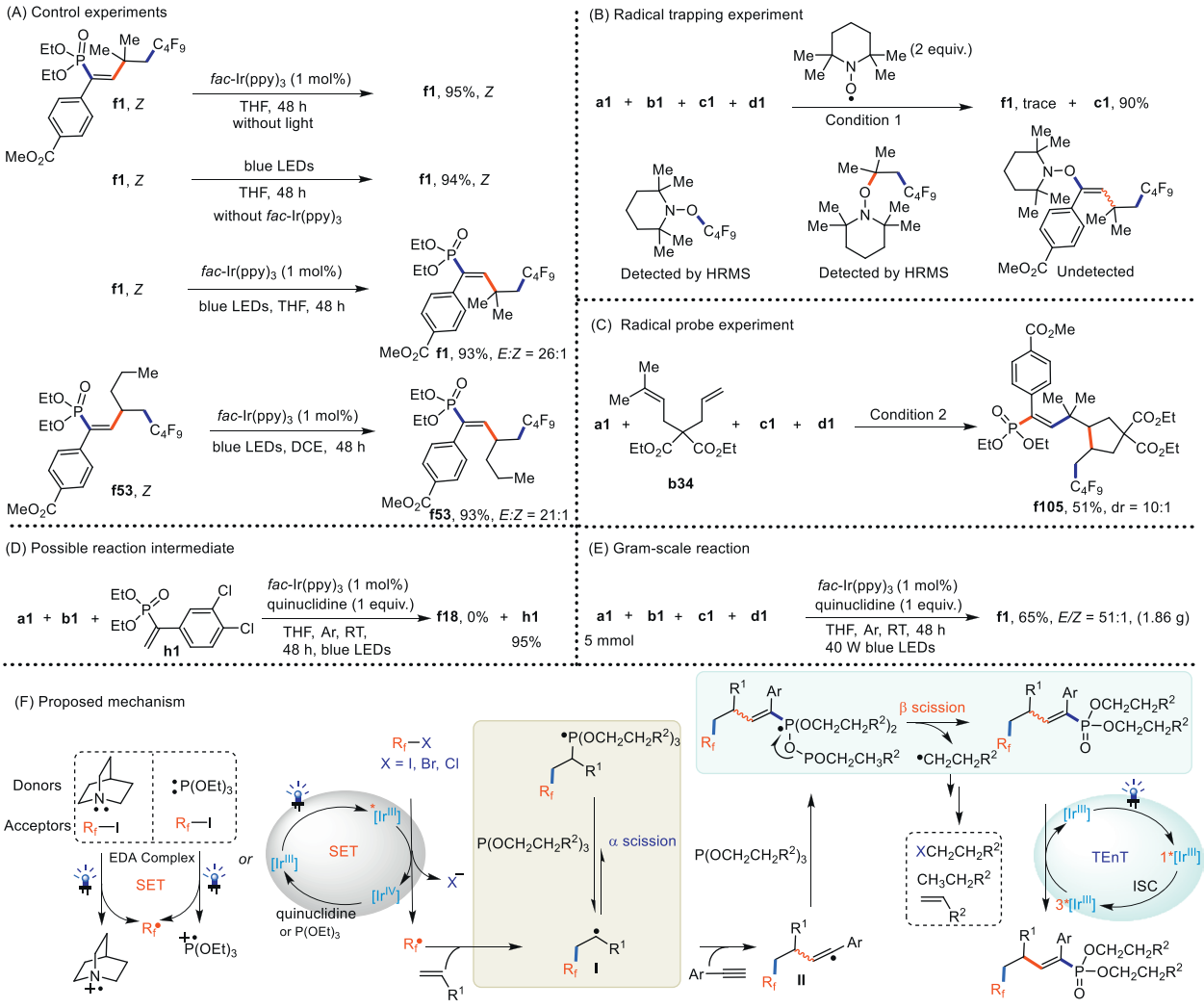


Fig. 5. Mechanism studies. (A) Control experiments. (B) Radical trapping experiment. (C) Radical probe experiment. (D) Possible reaction intermediate. (E) Gram-scale reaction. (F) Proposed mechanism.

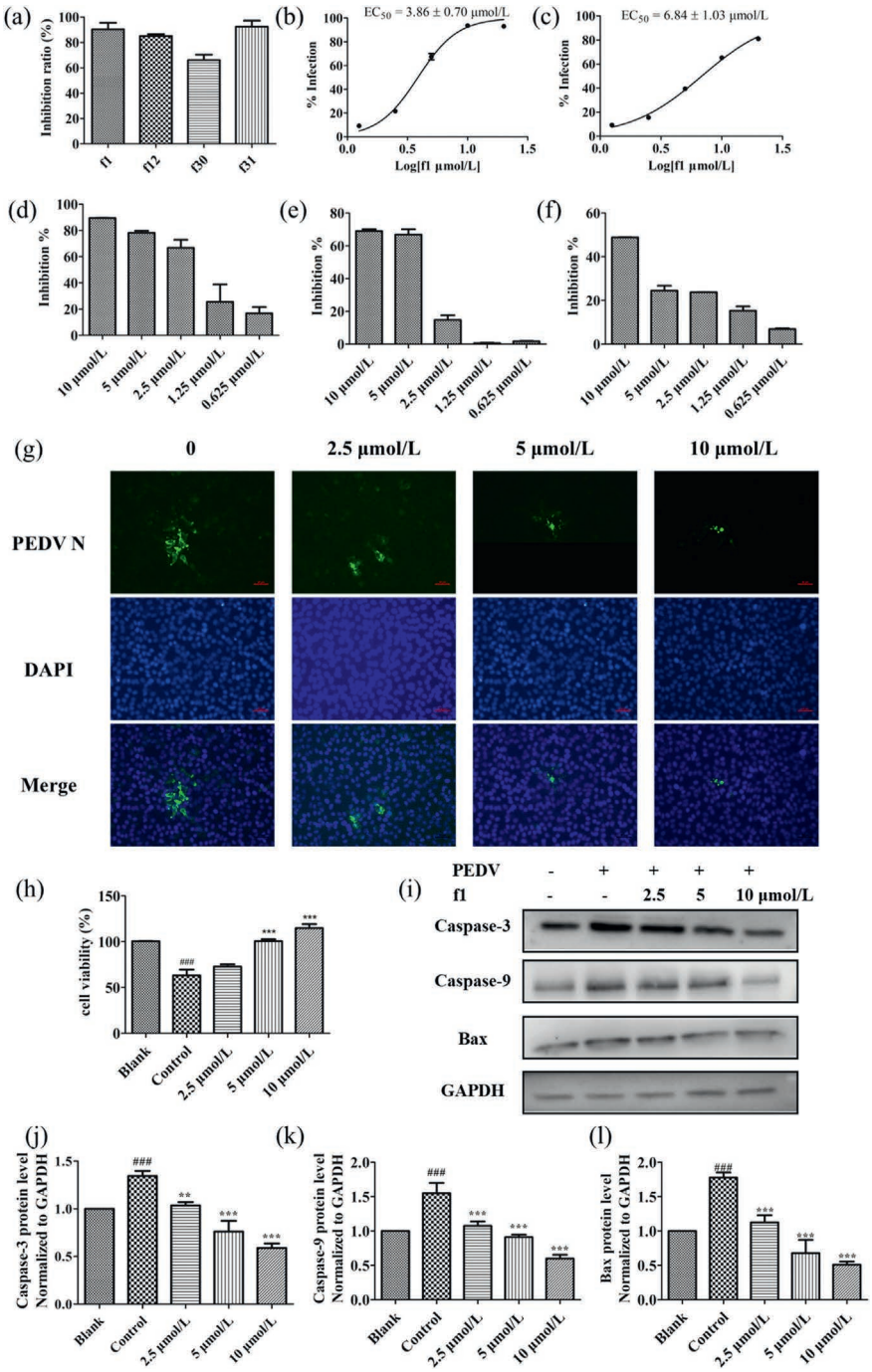


Fig. 6. Investigations into the antiviral activity of selected products. (a) Inhibition of PEDV by **f1**, **f12**, **f30**, and **f31** at 10 μmol/L in Vero-E6 cells. Antiviral activity of **f1** against the PEDV strain in Vero-E6 (b) or IPEC-J2 (c) cells. The inhibitory effect of **f1** on PEDV virus replication (d), invasion (e) and adsorption (f) in Vero-E6 cells. (g) The IFA analysis of the inhibitory effects of **f1** on the expression of N protein in PEDV infected Vero-E6 cells. (h) Effect of different doses of **f1** on apoptosis in PEDV-infected cells. (i-l) The effect of **f1** on the signaling pathway related to apoptosis. Error bars indicate means ± SD. $^{###}P < 0.001$, compared with the blank group; * $P < 0.05$, ** $P < 0.01$, *** $P < 0.001$, compared with the control group.

sequent controlled experiments demonstrate that the photocatalyst and light are essential for regulating the olefin configuration (Fig. 5A). Without either light or *fac*-Ir(ppy)$_3$, the conversion of alkenyl phosphonates from the *Z* configuration to the *E* configuration is not feasible. However, this transformation can be readily accomplished when both light and *fac*-Ir(ppy)$_3$ are present. Consequently, the *Z*/*E* selectivity is achieved through TEnT between the photoexcited *fac*-Ir(III)* and the alkenyl phosphonates [50–53]. The reaction proceed *via* a radical process, as complete inhibition was observed when TEMPO was employed as a radical quenching agent and the adducts formed between TEMPO and the fluoroalkyl/alkyl radicals were detected through high-resolution mass spectrometry (HRMS) (Fig. 5B). The TEMPO adduct of the vinyl radical II was not detected in this reaction. The high affinity of TEMPO for fluoroalkyl/alkyl radicals likely precludes their addition to alkynes, accounting for the absence of TEMPO-vinyl radical adducts. Furthermore, the radical process was corroborated through "radical clock" experiments, and the cyclization product **f105** was easily synthesized under the standard condition (Fig. 5C) [74]. Additionally, it has been reported that alkyl phosphites readily react with aryl

alkynes in photoreactions to produce corresponding Michael-type alkenyl phosphates [75]. To investigate whether the reaction proceeds *via* a Michael-type intermediate, we synthesized the relevant Michael-type alkenyl phosphate ester **h1** and employed it as a substitute for both alkynes and alkyl phosphite esters. Nevertheless, no target product formed (Fig. 5D). A gram-scale reaction was conducted to evaluate the feasibility of this approach, leading to the successful synthesis of the model product **f1** with satisfactory yield and high *Z*/*E* selectivity (Fig. 5E). According to the above investigations and literatures, a proposed mechanism is depicted in Fig. 5F. The reaction is initiated through two pathways: the single-electron reduction of perfluorobutyl iodide by photoexcited Ir(III)* and the photoinitiation of an EDA adduct between perfluorobutyl iodide and quinuclidine or $P(OEt)_3$. Subsequently, the distinct reactivity of alkyl phosphites toward different carbon radicals enables the chemoselective tandem additions of the fluoroalkyl radical to alkenes and arylalkynes [28–35]. Finally, the *Z*/*E* selectivity of the forming vinylphosphonates is further regulated by photoexcited Ir(III)* through TEnT [50–53].

Inspired by the diverse biological activities of fluorinated phosphonates [26–27,54], we evaluated the antiviral activities of these structurally unique δ-fluoroalkyl-substituted alkenyl phosphonates (Fig. 6). First, the products were screened for anti-PEDV activity in Vero-E6 cells, in which, compounds **f1**, **f12**, **f30**, **f31** showed potent activities against PEDV with inhibition rates of 93.05%, 83.94%, 75.17%, 99.47%, respectively (Fig. 6a). Given that **f1** showed low cytotoxicity (CC_{50} > 100 μmol/L), it was selected for follow-up studies (Fig. S5 in Supporting information). Compound **f1** was observed to inhibit PEDV replication in Vero-E6 cells with EC_{50} values of 3.86 ± 0.71 μmol/L (Fig. 6b). Due to the primary infection and replication of PEDV in small intestinal enterocytes, the *in vitro* antiviral activities of **f1** against PEDV were evaluated using IPEC-J2 cells. **f1** showed remarkable antiviral activities ($EC_{50} = 6.84 \pm 1.03$ μmol/L) and low cytotoxicity ($CC_{50} = 950.1 \pm 5.31$ μmol/L) (Fig. 6c and Fig. S5). To investigate the mechanism by which **f1** inhibits PEDV, we introduced **f1** to the virus during the adsorption, invasion, and replication stages, respectively. As shown in Figs. 6d-f, **f1** exhibits inhibitory capabilities against the viral adsorption, entry, and replication phases, with a primary and dose-dependent suppression focused on the replication phase. Additionally, **f1** effectively inhibits viral adsorption at high concentrations.

In addition, an indirect immunofluorescence assay was conducted to verify the antiviral effects [76–77]. As shown in Fig. 6g, **f1** inhibited the multiplication of PEDV in a dose-dependent manner in IPEC-J2 cells compared to the drug-free mock cells. Prior studies have demonstrated that PEDV induces caspase-3-mediated apoptosis in the late stages of infection, which may significantly contribute to cytotoxicity and pathogenesis [78–79]. Given the critical role of virus-induced apoptosis in the replication and pathogenesis of PEDV, an anti-apoptotic intervention may offer a rational approach for the development of targeted therapies [80,81]. Therefore, the anti-apoptotic activity of **f1** was investigated *in vitro*. As in Figs. 6h-l, **f1** inhibited the PEDV-induced apoptosis, and the levels of Bax, Caspase-3, and Caspase-9 were decreased in a dose-dependent manner. The above results exhibited that **f1** can inhibit cell apoptosis induced by PEDV *in vitro,* and the inhibition is dose-dependent.

In conclusion, a dual photocatalytic radical 1,4-difunctionalization strategy has been developed through alkyl phosphite-mediated radical cascade addition across ordinary alkenes and arylacetylenes. The challenging issue of *Z*/*E* selectivity control in the reaction of vinyl radicals with phosphite has been effectively addressed by integrating photocatalyzed SET and TEnT processes. Various structurally significant δ-fluoroalkyl-substituted vinyl phosphates have been rapidly synthesized with high *Z*/*E* selectivity under mild conditions. Furthermore, we discovered a new chemotype of lead compounds against PEDV from products. Preliminary studies suggested these compounds exhibit an unusual synergistic inhibitory effect on PEDV. They can effectively block the virus's attachment, entry, and replication, and attenuate PEDV-induced cell apoptosis *in vitro*. These findings are expected to accelerate the development of novel multifunctional antiviral medications. In addition, we generally evaluate the value of a new synthetic methodology by synthesizing or modifying the known drugs or bioactive molecules. However, in this work, we discovered a new chemotype of multifunctional antiviral compounds through designing a photocatalytic multicomponent reaction using readily accessible alkenes, arylacetylenes, perfluorobutyl iodide, and alkyl phosphites. Therefore, this study presents a vivid example of discovering new lead compounds by designing photocatalytic complexity-generating reactions. We hope this work will encourage new efforts to explore new photocatalytic radical multicomponent reactions.

Declaration of competing interest

The authors declare that they have no known competing financial interests or personal relationships that could have appeared to influence the work reported in this paper.

CRediT authorship contribution statement

Ruihua Liu: Writing – review & editing, Writing – original draft, Methodology, Investigation, Funding acquisition, Formal analysis, Data curation, Conceptualization. **Jiashu Chen:** Writing – original draft, Methodology, Investigation, Formal analysis, Data curation. **Nan Zhou:** Methodology, Investigation. **Cong Shi:** Methodology, Investigation. **Hongyun Qin:** Investigation. **Wenlong Shan:** Methodology. **Zemin Wang:** Writing – review & editing, Validation. **Chenxia Gao:** Investigation. **Chao Liu:** Methodology. **Bokan Wang:** Data curation, Conceptualization. **Chao Xie:** Investigation. **Xiangqian Li:** Writing – review & editing, Funding acquisition, Conceptualization. **Yuxi Lin:** Methodology. **Jiqiang Zhu:** Data curation. **Pan Xing:** Data curation. **Dayong Shi:** Writing – review & editing, Methodology, Conceptualization.

Acknowledgments

This work was supported by the National Natural Science Foundation of China (No. 22501160), the Natural Science Foundation for Youths of Shandong Province (No. ZR2022QB090), Key R&D Program of Shandong Province of China (No. 2023CXGC010413), Natural Science Foundation of Shandong Province (No. ZR2023MH245), Qingdao Emerging Industry Cultivation Project in 2023 (No. 23–1–4-xxgg-19-nsh), Shandong Provincial Science and Technology SME Innovation Capacity Improvement Project (No. 2025TSGCXTHG011). We thank Haiyan Sui, Xueyun Geng and Xiaoju Li of the Core Facilities for Life and Environmental Sciences, State Key laboratory of Microbial Technology of Shandong University for NMR.

Supplementary materials

Supplementary material associated with this article can be found, in the online version, at doi:10.1016/j.cclet.2025.112156.

References

[1] E. Ruijter, R. Scheffelaar, R.V.A. Orru, Angew. Chem. Int. Ed. 50 (2011) 6234–6246.
[2] A. Domling, W. Wang, K. Wang, Chem. Rev. 112 (2012) 3083–3135.
[3] C. Chen, X. Li, C.S. Neumann, et al., Angew. Chem. Int. Ed. 44 (2005) 2249–2252.

[4] X. Wu, C. Zhu, Acc. Chem. Res. 53 (2020) 1620–1636.
[5] T.D. Tan, J.M.I. Serviano, X. Luo, et al., Nat. Catal. 7 (2024) 321–329.
[6] H. Jiang, A. Studer, Chem. Soc. Rev. 49 (2020) 1790–1811.
[7] A. Studer, D.P. Curran, Angew. Chem. Int. Ed. 55 (2015) 58–102.
[8] H. Yi, G. Zhang, H. Wang, et al., Chem. Rev. 117 (2017) 9016–9085.
[9] J. Xuan, A. Studer, Chem. Soc. Rev. 46 (2017) 4329–4346.
[10] U. Wille, Chem. Rev. 113 (2012) 813–853.
[11] B. Giese, Angew. Chem. Int. Ed. 22 (1983) 753–764.
[12] B.P. Roberts, Chem. Soc. Rev. 28 (1999) 25–35.
[13] F. Parsaee, M.C. Senarathna, P.B. Kannangara, et al., Nat. Rev. Chem. 5 (2021) 486–499.
[14] A. Ruffoni, R.C. Mykura, M. Bietti, et al., Nat. Synth. 1 (2022) 682–695.
[15] J.J.A. Garwood, A.D. Chen, D.A. Nagib, J. Am. Chem. Soc. 146 (2024) 28034–28059.
[16] L. Shi, Univ. Chem. 39 (2024) 131–135.
[17] G. Tan, F. Paulus, Á. Rentería-Gómez, et al., J. Am. Chem. Soc. 144 (2022) 21664–21673.
[18] G. Tan, F. Paulus, A. Petti, et al., Chem. Sci. 14 (2023) 2447–2454.
[19] S.S. Li, Y.S. Jiang, X.L. Luo, et al., Sci. China Chem. 67 (2024) 558–567.
[20] C. Ascenzi Pettenuzzo, D.R. Pradhan, J. Singh, et al., J. Am. Chem. Soc. 147 (2025) 10382–10390.
[21] H. Jiang, G. Seidler, A. Studer, Angew. Chem. Int. Ed. 58 (2019) 16528–16532.
[22] Y. Zhang, K.D. Li, C.Q. Zhou, et al., Green Chem. 26 (2024) 10434–10440.
[23] J.C. Lo, J. Gui, Y. Yabe, et al., Nature 516 (2014) 343–348.
[24] J.C. Lo, Y. Yabe, P.S. Baran, J. Am. Chem. Soc. 136 (2014) 1304–1307.
[25] H.Y. Tu, S. Zhu, F.L. Qing, Chem. Commun. 54 (2018) 12710–12713.
[26] G.P. Horsman, D.L. Zechel, Chem. Rev. 117 (2016) 5704–5783.
[27] U. Pradere, E.C. Garnier-Amblard, S.J. Coats, et al., Chem. Rev. 114 (2014) 9154–9218.
[28] W.G. Bentrude, Acc. Chem. Res. 15 (1982) 117–125.
[29] A.K. Bhattacharya, Chem. Rev. 81 (1981) 415–430.
[30] X.Y. Jiao, W.G. Bentrude, J. Am. Chem. Soc. 121 (1999) 6088–6089.
[31] X.Y. Jiao, W.G. Bentrude, J. Org. Chem. 68 (2003) 3303–3306.
[32] N.B. Bissonnette, N. Bisballe, A.V. Tran, et al., J. Am. Chem. Soc. 146 (2024) 7942–7949.
[33] D. Reich, A. Noble, V.K. Aggarwal, Angew. Chem. Int. Ed. 61 (2022) e202207063.
[34] J. Yin, X. Lin, L. Chai, et al., Chem 9 (2023) 1945–1954.
[35] K. Sedillo, F. Fan, R.R. Knowles, et al., J. Am. Chem. Soc. 146 (2024) 20349–20356.
[36] E.L. Cochran, F.J. Adrian, V.A. Bowers, J. Chem. Phys. 40 (1964) 213–220.
[37] R.W. Fessenden, J. Chem. Phys. 71 (1967) 74–83.
[38] R.M. Kopchik, J.A. Kampmeier, J. Am. Chem. Soc. 90 (1968) 6733–6741.
[39] W. Shan, Z. Wang, C. Gao, et al., Green Chem. 26 (2024) 9749–9756.
[40] R. Liu, Y. Tian, J. Wang, et al., Sci. Adv. 8 (2022) eabq8596.
[41] Z. Wang, C.X. Yan, R. Liu, et al., Sci. Bull. 69 (2024) 345–353.
[42] H. Qin, R. Liu, Z. Wang, et al., Angew. Chem. Int. Ed. 64 (2024) e202416923.
[43] F. Wang, D. Wang, X. Wan, et al., J. Am. Chem. Soc. 138 (2016) 15547–15550.
[44] W. Wu, Y. You, Z. Weng, Chin. Chem. Lett. 33 (2022) 4517–4530.
[45] X.Y. Dong, J.T. Cheng, Y.F. Zhang, et al., J. Am. Chem. Soc. 142 (2020) 9501–9509.
[46] F.L. Qing, X.Y. Liu, J.A. Ma, et al., CCS Chem. 4 (2022) 2518.
[47] T. Chatterjee, N. Iqbal, Y. You, et al., Acc. Chem. Res. 49 (2016) 2284–2294.
[48] J. Liu, X. Tao, Z. Zou, et al., Chin. Chem. Lett. 36 (2025) 110461.
[49] D. Leifert, A. Studer, Angew. Chem. Int. Ed. 59 (2020) 74–108.
[50] J.J. Molloy, J.B. Metternich, C.G. Daniliuc, et al., Angew. Chem. Int. Ed. 57 (2018) 3168–3172.
[51] J.J. Molloy, T. Morack, R. Gilmour, Angew. Chem. Int. Ed. 58 (2019) 13654–13664.
[52] A. Singh, C.J. Fennell, J.D. Weaver, Chem. Sci. 7 (2016) 6796–6802.
[53] K. Singh, S.J. Staig, J.D. Weaver, J. Am. Chem. Soc. 136 (2014) 5275–5278.
[54] V.D. Romanenko, V.P. Kukhar, Chem. Rev. 106 (2006) 3868–3935.
[55] J. Cui, F. Li, Z.L. Shi, Nat. Rev. Microbiol. 17 (2018) 181–192.
[56] J. Chen, Y. Lin, C. Gao, et al., J. Adv. Res. 80 (2026) 1009–1030.
[57] T.N. Shamsi, J. Yin, M.E. James, et al., Protein Pept. Lett. 29 (2022) 392–407.
[58] M. Wu, D. Yi, Q. Zhang, et al., Sci. Rep. 11 (2021) 6552.
[59] K. Jung, L.J. Saif, Vet. J. 204 (2015) 134–143.
[60] C. Liu, J. Tang, Y. Ma, et al., J. Virol. 89 (2015) 6121–6125.
[61] H. Chu, Y. Hou, D. Yang, et al., Nature 609 (2022) 785–792.
[62] L. Zhang, D. Lin, X. Sun, et al., Science 1979 368 (2020) 409–412.
[63] M. Liu, B. Lu, Y. Li, et al., Sig. Transduct. Target. Ther. 8 (2023) 385.
[64] Y. Zhu, F. Feng, G. Hu, et al., Nat. Commun. 12 (2021) 961.
[65] H.J. Dong, Z.H. Wang, W. Meng, et al., Viruses. 10 (2018) 601.
[66] Y. Yi, M. Zhang, H. Xue, et al., Acta Pharm. Sin. B 12 (2022) 4154–4164.
[67] J.H. Lee, J.S. Park, S.W. Lee, et al., Virus. Res. 195 (2015) 148–152.
[68] L. Yuan, S. Zhang, Y. Wang, et al., J. Virol. 92 (2018) e00809–e00818.
[69] Y. Cheng, S. Yu, Org. Lett. 18 (2016) 2962–2965.
[70] D. Wei, T. Liu, Y. He, et al., Angew. Chem. Int. Ed. 60 (2021) 26308–26313.
[71] J. Zhang, Y. Li, R. Xu, et al., Angew. Chem. Int. Ed. 56 (2017) 12619–12623.
[72] N. Iqbal, J. Jung, S. Park, et al., Angew. Chem. Int. Ed. 53 (2014) 539–542.
[73] G. Roh, N. Iqbal, E.J. Cho, Chin. J. Chem. 34 (2016) 459–464.
[74] D. Guilder, K.U. Ingold, Acc. Chem. Res. 13 (1980) 317–323.
[75] H. Wang, Q. Lu, C.W. Chiang, et al., Angew. Chem. Int. Ed. 56 (2016) 595–599.
[76] W.T. Qiao, X. Yao, W.H. Lu, et al., Int. J. Biol. Macromol. 270 (2024) 132408.
[77] M. Wang, C. Wu, N. Liu, et al., Eng. Microbio. 4 (2024) 100162.
[78] Y. Kim, C. Lee, Virology 460-461 (2014) 180.
[79] X. Zhang, P. Li, Q. Zheng, et al., Vet. Microbiol. 229 (2019) 159–167.
[80] Y. Chen, Z. Zhang, J. Li, et al., Virol. J. 15 (2018) 170.
[81] R.H. Lathakumari, L.K. Vajravelu, A. Gopinathan, et al., Eng. Microbio. 5 (2025) 100191.